RESEARCH

Compromised C3b-VSIG4 axis between decidual NK cells and macrophages contributes to recurrent spontaneous abortion

Siao Chen[1,2], Jinghe Zhang[1,2,3], Jian Chen[1,2,4], Jieqi Ke[1,2,3], Yu Huang[2,5], Xianghui Du[1,2,3], Binqing Fu[1,2,3*] and Haiming Wei[1,2,3*]

Abstract

NK cells and macrophages constitute the predominant immune cell subsets in the decidua during the first trimester of pregnancy, with macrophages typically adopting an anti-inflammatory phenotype. Conversely, in the third trimester, macrophages undergo a shift towards a pro-inflammatory phenotype concurrent with a reduction in NK cell numbers. The direct regulatory impact of NK cells on macrophage phenotype remains poorly explored. In our investigation, we observed that ICAM1^{+} macrophages stimulate the expression of intracellular C3 in LFA1^{+} decidual NK cells. Notably, Cathepsin W within NK cells exhibit the potential to generate active C3b fragments, effectively inhibit the proinflammatory phenotype of macrophages by binding to VSIG4. Our study unveils a direct regulatory mechanism orchestrated by decidual NK cells over macrophages, providing a potential pathogenic explanation for recurrent spontaneous abortion.

Keywords Decidual natural killer cell, Macrophage, Recurrent spontaneous abortion, Complement, VSIG4

*Correspondence:
Binqing Fu
fbq@ustc.edu.cn
Haiming Wei
ustcwhm@ustc.edu.cn
[1] Department of Life Sciences and Medicine, University of Science and Technology of China, 443 Huangshan Road, Hefei 230027, Anhui, China
[2] Institute of Immunology, University of Science and Technology of China, Hefei, Anhui, China
[3] Department of Obstetrics and Gynecology, Division of Life Sciences and Medicine, The First Affiliated Hospital of USTC, University of Science and Technology of China, Hefei, Anhui, China
[4] Department of Intensive Care Unit, Division of Life Sciences and Medicine, The First Affiliated Hospital of USTC, University of Science and Technology of China, Hefei, Anhui, China
[5] Division of Molecular Medicine, Hefei National Laboratory for Physical Sciences at Microscale, The CAS Key Laboratory of Innate Immunity and Chronic Disease, School of Life Sciences, University of Science and Technology of China, Hefei, Anhui, China

Background

Decidual natural killer (NK) cells constitute the predominant leukocyte population during the first trimester, representing approximately 70% of maternal interface leukocytes [1, 2]. With their unique CD56^{bright} CD16$^-$ phenotype distinct from peripheral natural killer cells [3], decidual natural killer cells exhibit high cytokine secretion capability and low cytotoxicity [4, 5], playing a crucial role in establishing immune tolerance at the maternal–fetal interface and promoting embryonic development [6]. The insufficient quantity and abnormal function of decidual natural killer (dNK) cells can both lead to adverse pregnancy outcomes [7, 8]. Macrophages, comprising approximately 20% of the total leukocytes within the human decidua, constitute the second-largest leukocyte population and play essential roles in establishing a compatible local immune balance [9–11]. Decidual macrophages are influenced by their local microenvironment

Chen *et al. Journal of Translational Medicine*   (2024) 22:1017

Page 2 of 18

at the maternal–fetal interface in a similar way to other tissue-resident macrophages [10].

Previous investigations have revealed dynamic changes in the phenotype of decidual macrophages throughout pregnancy. During the early stages, pro-inflammatory macrophages establish a mildly inflammatory environment in the endometrium that facilitates embryo implantation. In the second trimester, a shift to anti-inflammatory macrophages ensues, fostering immune tolerance and creating a stable milieu for embryonic development. As pregnancy progresses into the third trimester, macrophages undergo a reversion to the pro-inflammatory phenotype, playing a role in initiating labor [12, 13].

Several mechanisms have been documented to elucidate the transition of macrophages from pro-inflammatory to anti-inflammatory phenotypes. Decidual immune cells and the placenta exert an indirect inhibitory effect on the production of pro-inflammatory macrophages by secreting soluble inhibitory cytokines [14–16]. Additionally, trophoblasts secrete soluble decorin, which serves to inhibit M1 macrophages [17].

The temporal shift in the number of NK cells aligns with the timing of phenotypic transition in macrophages [18]. However, the existence of a direct inhibitory effect of NK cells on pro-inflammatory macrophages remains unreported. Investigation is needed to determine whether NK cells can bind to surface receptors on macrophages, inhibiting pro-inflammatory macrophages through this interaction.

Previous studies have primarily focused on how other cells within the decidual immune microenvironment, such as macrophages and T cells, regulate NK cells, while the regulatory effects of NK cells on other cell types have received comparatively less attention. Additionally, research on macrophage polarization has largely centered on the role of soluble factors, with limited exploration of the direct mechanisms involved in macrophage polarization. In this study, by examining the phenotypes of decidual NK cells and macrophages in women with normal pregnancies and those with recurrent spontaneous abortions, as well as establishing an in vitro co-culture system of macrophages and dNK cells, we identified that decidual NK cells regulate macrophage polarization through cell surface receptor-ligand interactions. Additionally, our study revealed the presence of an intracellular complement system in decidual NK cells, which plays a critical role in maintaining pregnancy homeostasis. These investigations underscore the pivotal role of decidual NK cells intracellular C3 in maintaining the normal decidual microenvironment, providing insights into the biology of the intracellular complement system and the pathogenesis of recurrent spontaneous abortion.

Methods

Human samples

Peripheral blood mononuclear cells (PBMCs) were obtained at the Blood Center of Anhui Province (Hefei, China). Informed consent was obtained from each donor. First-trimester decidual samples from normal pregnancies and recurrent spontaneous abortion were obtained at the First Affiliated Hospital of the University of Science and Technology of China (Hefei, China). Samples with the following conditions were strictly excluded: genetic abnormalities, uterine malformations, vaginal infections, antiphospholipid antibody syndrome or severe inflammation. All human samples used in the present study were obtained under the approval of the Ethics Committee of the University of Science and Technology of China (2022KY-015; Hefei, China).

Human sample isolation

Peripheral blood mononuclear cells (PBMCs) were isolated using Ficoll density gradients following established protocols. Decidual tissue was sheared and enzymatically digested with 2 mg/mL collagenase IV (Sigma, cat: C5138), and the digestion solution was filtered through a 70 µm cell strainer to obtain a cell suspension. The cell suspension was centrifuged at $600 \times g$ for 10 min to obtain a cell pellet. The cell pellet was resuspended in red blood cell lysis buffer (Biolegend, cat: 420301) and left at RT for 5 min to facilitate lysis. The lysed cell suspension was diluted with PBS to halt the lysis process. The suspension was centrifuged once again at $600 \times g$ for 10 min. The cell pellet was resuspended in culture medium. Decidual NK cells and macrophages were sorted from the obtained cell suspension using fluorescence-activated cell sorting (FACS) based on specific cell markers.

Fluorescence-activated cell sorting

Decidual single-cell suspensions were obtained as previously described in the methods section. Anti-CD14 antibodies were employed for macrophage staining [19], while anti-CD56 antibodies were utilized for NK cell staining. Antibody cocktails were applied to the cell suspensions and incubated for 30 min at 4 °C. The cells were washed twice with cold PBS and sorted by flow cytometry (FACSAria™ III Cell Sorter; BD Biosciences).

Flow cytometry

Monocyte-derived macrophages or decidua single cells were resuspended in 100 µL of PBS containing the antibody cocktail, and the cells were incubated for 30 min at 4 °C. The cells were washed twice with cold PBS and

Chen *et al. Journal of Translational Medicine*   (2024) 22:1017

Page 3 of 18

investigated by flow cytometry (FACSCelesta™ Cell Analyzer; BD Biosciences).

Fluorescent multiplex immunohistochemistry

Decidual tissue specimens from normal pregnancies and RSA patients were immersed in a 10% formaldehyde solution for fixation. Paraffin-embedded decidua tissues were sliced into 5 μm thick sections and mounted on glass. After deparaffinization and antigen retrieval of the sections, immunohistochemical staining was performed to identify specific cell populations by using a Tyramide SuperBoost™ Kit (Thermo Scientific, cat: B40912 &B40926) according to the manufacturer's instructions. Anti-CD68 antibodies (CST, cat: 76437S) were used to label decidual macrophages, and anti-CD56 antibodies (CST, cat: 3576S) were used to label decidual NK cells.

Immunohistochemistry

IHC staining was performed on consecutive decidual sections. Deparaffinization, hydration, and antigen retrieval were performed as described in the preceding text. Immunohistochemical staining was performed using a mouse or rabbit polymer detection kit (ZSGB-Bio, cat: PV-6001/PV-6002) following the manufacturer's instructions. An appropriate volume of an endogenous peroxidase enzyme inhibitor was added to the tissue sections. The sections were incubated at RT for 10 min. Subsequently, the sections were washed three times with PBS buffer, with each wash lasting 3 min. Depending on the size of the tissue sections, 100 μL or an appropriate volume of the primary antibody (the same antibodies as described above) was applied. The sections were incubated at 4 °C overnight. After primary antibody incubation, the sections were washed three times with PBS buffer, with each wash lasting 3 min. One hundred microliters or an appropriate volume of the enzyme-labeled goat anti-rabbit/mouse IgG polymer was applied to the sections. The sections were incubated at 37 °C for 20 min. Following this step, the sections were washed three times with PBS buffer, with each wash lasting 3 min. Freshly prepared DAB chromogenic solution (CST, cat: 8059S) was added to the sections. The sections were incubated at RT until positive signals appeared. A brief incubation (20 s) in hematoxylin staining solution was performed. Differentiation and rinsing continued until blue coloration was achieved.

Double-staining IHC

HRP and AP dual enzyme staining was performed on the same decidual section. Sample preprocessing was carried out following the standard procedures used in conventional IHC. The anti-CD56 (CST, cat: 3576S) antibody was labeled with alkaline phosphatase (AP) using the universal SAP kit (ZSGB-Bio, cat: SAP-9100) and visualized using Fast Red chromogenic substrate (ZSGB-Bio, cat: ZLI-9045). The labeled NK cells were observed as red staining. The anti-CD68 antibody was labeled with horseradish peroxidase (HRP) and visualized using DAB chromogenic substrate as described. The labeled macrophages were observed as brown staining.

Viable cell labeling and coincubation

Decidual NK cells or macrophages were suspended at a concentration of 1×10^6/mL in RPMI 1640 serum-free culture medium. For every milliliter of cell suspension, 5 μL of the provided cell-labeling solution (Thermo, cat: V22889) was added, and thorough mixing was achieved through gentle pipetting. Incubation was conducted at 37 °C for 15 min. The labeled suspension tubes were subjected to centrifugation at $300\times g$ for 5 min. The supernatant was carefully aspirated, and the cells were gently resuspended in warm (37 °C) RPMI 1640 medium. The washing procedure was repeated two additional times. Decidual NK cells and macrophages, following completion of labeling, were resuspended in 200 μL of RPMI 1640 complete medium. The cell suspension was then placed in a cell culture incubator set at 37 °C with 5% CO_2 for 1 h. After the incubation period, 2 mL of 4% paraformaldehyde (PFA) was added to the cell suspension for fixation, and the cells were incubated for 20 min at RT. The fixed cell suspension was then centrifuged at 2000 rpm for 10 min. Following centrifugation, the cell pellet was resuspended in 50 μL of PBS and gently mixed for subsequent fluorescence imaging.

Quantitative PCR analysis

Total RNA was prepared using TsingZol Reagent (Tsingke, cat: TSP401) and reverse-transcribed into complementary (c) DNA using MonScript™ RTIII All-in-One Mix with dsDNase (Monad, cat: MR05101M). Specific primers were designed for target genes, and the relative gene expression levels in cDNA samples were assessed using real-time quantitative reverse transcription-polymerase chain reaction (RT–PCR) with the SYBR Green Premix Pro Taq HS qPCR Kit (Accurate Biology, cat: AG11746). To normalize gene expression data, β-actin was employed as an endogenous control. The primers utilized are listed in Table S2.

Macrophage polarization

The induction method of macrophages was based on the previous studies [20, 21]. Monocytes were resuspended in RPMI 1640 complete medium (10% FBS and penicillin–streptomycin solution), and human M-CSF was added at a final concentration of 50 ng/mL. 1 mL of cell suspension was plated into each well of a 6-well culture

Chen *et al. Journal of Translational Medicine*   (2024) 22:1017

Page 4 of 18

plate. Subsequently, half of the medium was changed every other day to induce differentiation for 6–7 days, resulting in the differentiation of cells into the M0 phenotype. After 6–7 days of differentiation, 100 ng/mL LPS and 20 ng/mL human IFN-γ were added while maintaining the presence of human M-CSF. Polarize for 24 h to obtain M1 macrophages. After 6–7 days of differentiation, 20 ng/ml human IL-4 was added while maintaining the presence of human M-CSF. Polarize for 24 h to obtain M2 macrophages.

Coculture system of monocyte-derived macrophage (MdM)—dNK cells

Following the aforementioned steps, monocytes were induced to differentiate into M1/M2 macrophages. Subsequently, a five-fold excess of decidual NK cells was added, and centrifugation at 200×*g* for 2 min was performed to facilitate the settling of NK cells at the bottom of the well plate, ensuring improved interaction with macrophages. After a 48-h incubation period, NK cells were removed due to their suspension properties, and the phenotypic changes in macrophages were assessed. Inducers of M1/M2 macrophages were present throughout this process.

Antibody blockade of VSIG4

To block the signal transduction of the C3b-VSIG4 axis, an anti-human VSIG4 blockade antibody (R&D, cat: MAB46462) was added at a concentration of 50 μg/mL before NK cells were added to the MdM-dNK cell coculture system.

Molecular docking

Protein–protein docking is used to predict the C3 (PDB ID: 2A73) and CTSW (Predicted by alphafold2) heterodimer. Rigid-body docking was performed using ZDOCK [22]. A total of 2000 poses were generated, and the poses with the highest scores for the receptor–ligand complexes were retained for further analysis. The best binding pose was filtered by PDBePISA online server (https://www.ebi.ac.uk/pdbe/pisa/) with macromolecular interfaces and interactions. Structural analysis and figure preparation were carried out using PyMol (https://pymol.org).

Western blot

Lysates of decidual NK cells were prepared using RIPA lysis buffer (Thermo Scientific, cat: 89900) supplemented with ProtLytic protease inhibitor cocktail (NCM Biotech, cat: P001). After centrifugation (14,000×*g*, 10 min, 4 °C), supernatants were collected for sodium dodecyl sulfate–polyacrylamide gel electrophoresis. Then, proteins were transferred to polyvinylidene difluoride (PVDF) membranes and blocked with QuickBlock™ Blocking Buffer (Beyotime, cat: P0252) for 15 min at RT. PVDF membranes were incubated with anti-C3 (Abcam, cat: ab200999) or anti-CTSW (Abcam, cat: ab191083) antibody overnight at 4 °C and then incubated with HRP-conjugated goat anti-rabbit IgG (Sangon Biotech, cat: D110058).

RNA sequencing

Peripheral blood NK cells, monocytes, decidual macrophages and NK cells from both normal pregnant individuals and patients with recurrent spontaneous abortion (RSA) were collected, and RNA was isolated using Tsing-Zol Reagent (Tsingke, cat: TSP401). Total amounts and integrity of RNA were assessed using the RNA Nano 6000 Assay Kit of the Bioanalyzer 2100 system (Agilent Technologies, CA, USA). Total RNA was used as input material for the RNA sample preparations. Briefly, mRNA was purified from total RNA by using poly-T oligo-attached magnetic beads. Fragmentation was carried out using divalent cations under elevated temperature in First Strand Synthesis Reaction Buffer (5X). First-strand cDNA was synthesized using random hexamer primers and M-MuLV Reverse Transcriptase, and then RNaseH was used to degrade the RNA. Second strand cDNA synthesis was subsequently performed using DNA Polymerase I and dNTPs. The remaining overhangs were converted into blunt ends via exonuclease/polymerase activities. After adenylation of the 3′ ends of DNA fragments, adaptors with hairpin loop structures were ligated to prepare for hybridization. To preferentially select cDNA fragments 370–420 bp in length, the library fragments were purified with the AMPure XP system (Beckman Coulter, Beverly, USA). Then, PCR amplification was performed, the PCR product was purified by AMPure XP beads, and the library was finally obtained. To ensure the quality of the library, the library needs to be tested. After the construction of the library, the library was initially quantified by Qubit2.0 The samples were then diluted to 1.5 ng/μL, and the insert size of the library was detected by an Agilent 2100 bioanalyzer. After the insert size met the expectation, qRT–PCR was used to accurately quantify the effective concentration of the library (the effective concentration of the library was higher than 2 nM) to ensure the quality of the library. After the library is qualified, the different libraries are pooling according to the effective concentration and the target amount of data off the machine, then being sequenced by the Illumina NovaSeq 6000. The end reading of 150 bp pairing is generated. The basic principle of sequencing is to synthesize and sequence at the same time (Sequencing by Synthesis). Four fluorescent labeled dNTP, DNA polymerase and splice primers were added to the sequenced flow cell and amplified. When the sequence cluster extends the

Chen *et al. Journal of Translational Medicine*   (2024) 22:1017

Page 5 of 18

complementary chain, each dNTP labeled by fluorescence can release the corresponding fluorescence. The sequencer captures the fluorescence signal and converts the optical signal into the sequencing peak by computer software, so as to obtain the sequence information of the fragment to be tested.

Gene set analysis

In order to investigate pathway differences between conditions, gene set analyses were performed with the cluster Profiler (version 4.10.0) [23]. R package after Bulk RNA-seq work flow, including Gene-set enrichment analysis (GSEA) and Gene Set Variation Analysis (GSVA). GSEA was utilized to investigate the enriched pathways associated with the upregulated and down-regulated genes between conditions, allowing for the identification of gene sets (KEGG pathway, for example) that show statistically significant, concordant differences between two biological states. Furthermore, GSVA was utilized to measure the sample-wise gene set enrichment scores for specific signatures (M1/M2-prone gene signature) [24], allowing for the detection of subtle pathway activity changes over a sample population in comparison to corresponding methods.

scRNA sequence analysis

The single-cell RNA sequencing data used in this study were previously published by Guo C et al. [9]. To examine the gene expression of ICAM and VSIG4 on macrophages of decidua tissues from both normal subjects and RSA patients, raw data were processed using Cell Ranger (Version 3.0.0) [25] against the GRCh37 human reference genome with default parameters. Subsequently, the Seurat pipeline was applied with default parameters (Seurat version 5.0.2) [26]. Data from different batches were integrated with the canonical correlation analysis (CCA) method implemented in Seurat.

Statistical analyses

Statistical significance was determined using Prism 8.0 (GraphPad, San Diego, CA, USA). Two-tailed unpaired Student' s t-tests were used to determine significance between two groups, unless otherwise specified as paired t-tests in the figure legends. Data represent the mean ± SD. $P < 0.05$ was considered significant.

Results

Reduced cell-to-cell interactions between decidual NK cells and macrophages in RSA patients.

To investigate potential direct interactions between decidual macrophages and NK cells through cell surface ligands, we employed anti-CD68 antibodies to label macrophages and anti-CD56 antibodies to label NK cells for in situ detection in decidual tissue (Fig. 1A). Both NK cells and macrophages are abundantly present in decidua from both normal individuals and those with recurrent spontaneous abortion (RSA). However, in the perivascular regions of decidual tissue from RSA patients, there is a significant reduction in the number of NK cells in close proximity to macrophages. To further elucidate this phenomenon, we performed staining for NK cells and macrophages on consecutive sections of decidual tissue (Fig. 1B). Using the same tissue structure for localization in two consecutive sections, in normal decidua, NK cells are snugly positioned within the gaps between macrophages. Conversely, in the decidua of RSA patients, NK cells are notably distant from macrophages. Additionally, we conducted double staining for both cell types on the same decidual tissue section, revealing a similar pattern (Fig. 1C). Statistical analysis of the distance between macrophages (brown) and the nearest NK cells (pink) in the field of view revealed a significantly greater nuclear spacing ($P < 0.0001$) in RSA patient decidual NK cells and macrophages compared to normal individuals (Fig. 1D). Images of each cell pair and the distances between their nuclei are shown in Figure S1 and Table S1.

Subsequently, decidual NK cells and macrophages sorted from both normal individuals and RSA patients were cocultured in vitro. Although the number of sorted cells was consistent with healthy controls, the number of NK cells positioned on the same focal plane as macrophages in RSA patient noticeably decreased, indicating a reduction in the interactions between these two cell types (Fig. 1E). Collectively, these findings suggest that the direct interaction between decidual NK cells and macrophages via cell membrane

(See figure on next page.)

Fig. 1 Reduced cell-to-cell interactions between decidual NK cells and macrophages in RSA patients. **A** Immunofluorescence staining demonstrating the co-localization of decidual NK cells and macrophages in situ in decidua tissues from normal pregnancies and RSA patients. Scale bar = 5 μm. **B** Representative immunohistochemical staining of CD68 and CD56 in the serial sections from the same normal pregnant woman or RSA patient. Scale bar = 5 μm. **C** Dual-color immunohistochemistry depicting cells expressing CD68 (pink) or CD56 (brown) within the same decidual tissue section. Scale bar = 10 μm. **D** Statistical analysis of cell-to-cell distances between NK cells and macrophages in decidual tissues from normal pregnancies (n = 3) and RSA patients (n = 3). Thirty cell pairs were randomly selected per tissue section. P values have been determined by two-tailed unpaired t-test. **E** Live cell fluorescence staining showing in vitro binding interactions between FACS-sorted decidual NK cells and macrophages from normal pregnancies or RSA patient. Scale bar = 5 μm
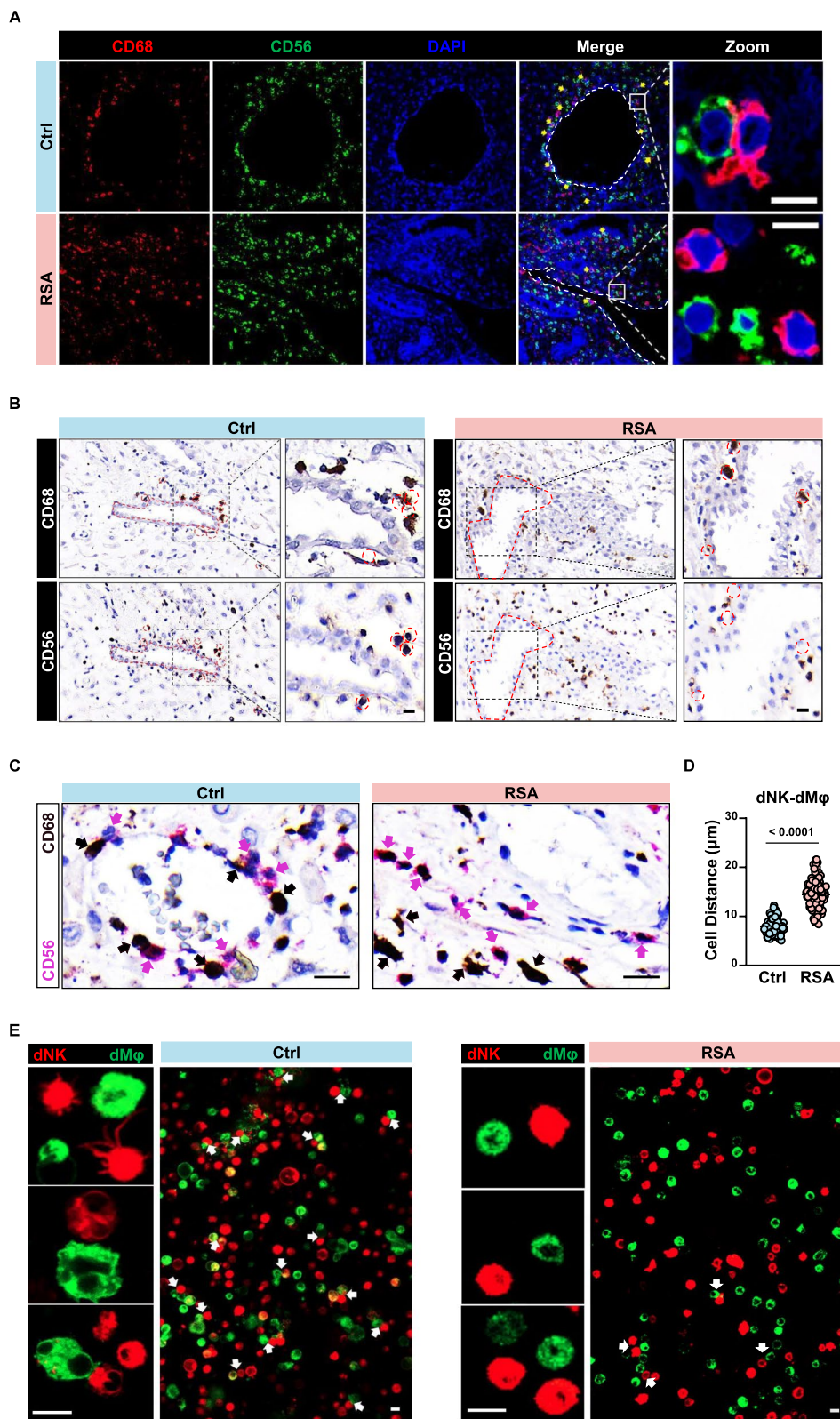
Chen *et al. Journal of Translational Medicine*   (2024) 22:1017

Page 6 of 18

Fig. 1 (See legend on previous page.)

Chen *et al. Journal of Translational Medicine*   (2024) 22:1017

Page 7 of 18

surface ligands may be more prevalent in normal pregnancy decidua, with a significant reduction observed in RSA patient decidua.

M1-prone gene expression signature in the decidual macrophages of RSA patients

To elucidate the phenotypic characteristics of decidual macrophages in individuals with recurrent spontaneous abortion (RSA) and those with normal pregnancies, we sorted decidual macrophages from both groups for RNA sequencing. The gating strategy of flow cytometry was shown in Figure S2. Heatmaps were generated to visualize the expression levels of previously reported M1 or M2 macrophage phenotype markers in these two macrophage populations [24]. Notably, the expression of M1 phenotype markers in decidual macrophages from RSA patients consistently exceeded that in macrophages from normal pregnant decidua, while the trend was reversed for M2 phenotype markers (Fig. 2A, B).

To complement our findings, we conducted an analysis of previously reported single-cell RNA-seq data for decidual macrophages [9] (Fig. 2C). Among the molecules significantly upregulated in RSA patient decidual macrophages compared to those from normal pregnancy, FCN1 [27], VCAN [28], S100A8, and S100A9 [29, 30] were reported as molecules associated with activated macrophages. Conversely, molecules such as TREM2 [31–33], CCL4 [34], and MMP9 [35], which exhibited lower expression, have been reported to be highly expressed in tumor-associated macrophages (TAMs). Furthermore, we employed GSVA analysis to assess M1- or M2-prone gene signatures within the RNA-sequence data. The results indicated a significantly higher M1-prone gene signature score in RSA decidual macrophages than in normal decidua, while the M2-prone gene signature score was significantly lower in RSA patient decidual macrophages (Fig. 2D, E). To validate these findings, we performed qPCR to assess the expression levels of selected M1 and M2 markers (Fig. 2F, G). M1 markers, including CD86, CD40, CCR7, and CXCL9, exhibited significantly increased expression in RSA patient decidual macrophages, whereas M2 markers, such as CLEC7A, CTSC, MMP9, and CCL4,

demonstrated marked downregulation in RSA patient decidual macrophages [24].

These results provide compelling evidence that decidual macrophages in RSA patients adopt an activated state, while those in normal pregnant decidua remain relatively quiescent.

dNK cells from normal pregnancy inhibit proinflammatory macrophages

To investigate whether the M1 phenotype inclination of decidual macrophages in RSA patients might be attributed to a lack of interaction with decidual NK cells, we initiated an experimental approach. Peripheral blood mononuclear cells (PBMCs) were isolated from human donors, and monocytes were induced with human M-CSF to generate M0 macrophages. After 7 days, the cells underwent morphological changes, transitioning into M0 macrophages. Subsequent stimulation with LPS/IFNγ or IL-4 led to the differentiation of M0 cells into M1 or M2 macrophages, respectively [20, 21]. Flow cytometry analysis revealed three distinct subpopulations characterized by the cell markers CD206 and CD80 (Fig. 3A, B).

To evaluate the impact of decidual NK cells on M1 macrophages, M1 macrophages were cocultured with normal decidual NK cells for 48 h. Following coculture, macrophages were harvested, and their phenotypes were assessed. Flow cytometry analysis showed a significant decrease in CD80 expression ($P = 0.0108$) and a notable increase in CD206 expression ($P = 0.0134$) in M1 macrophages after 48 h of coculture with dNK cells (Fig. 3C, D). However, these macrophages did not fully transition into M2 macrophages. Previous reports have indicated distinct morphological differences between M1 and M2 macrophages [36]. In essence, the elongation of macrophages is associated with increased expression of M2 polarization markers such as Arg-1, CD206, and YM-1, while M1-polarized macrophages generally exhibit an oval shape. Upon observation of M1 macrophages cocultured with normal dNK cells, it was evident that many previously oval-shaped cells had elongated, suggesting a phenotypic shift toward the M2 direction. In contrast, most M2 macrophages cocultured with dNK cells maintained their elongated morphology (Fig. 3E).

(See figure on next page.)

Fig. 2 M1-prone gene expression signature in RSA patients. **A**, **B** Heatmap showing expression levels of DEGs selected for known M1(A) or M2(B) gene markers in decidual macrophages sorted from normal pregnancies (n = 3) and RSA patients (n = 3). **C** Volcano plot showing DEGs in macrophages single cell sequencing from NP and RSA. **D**, **E** GSVA scores were calculated from the macrophages RNA-seq dataset using the gene lists indicated M1(D) and M2(E) phenotype. **F**, **G** Validation of M1 or M2 gene expression in normal macrophages and RSA patient macrophages through qPCR analysis. P values have been determined by two-tailed unpaired t-test
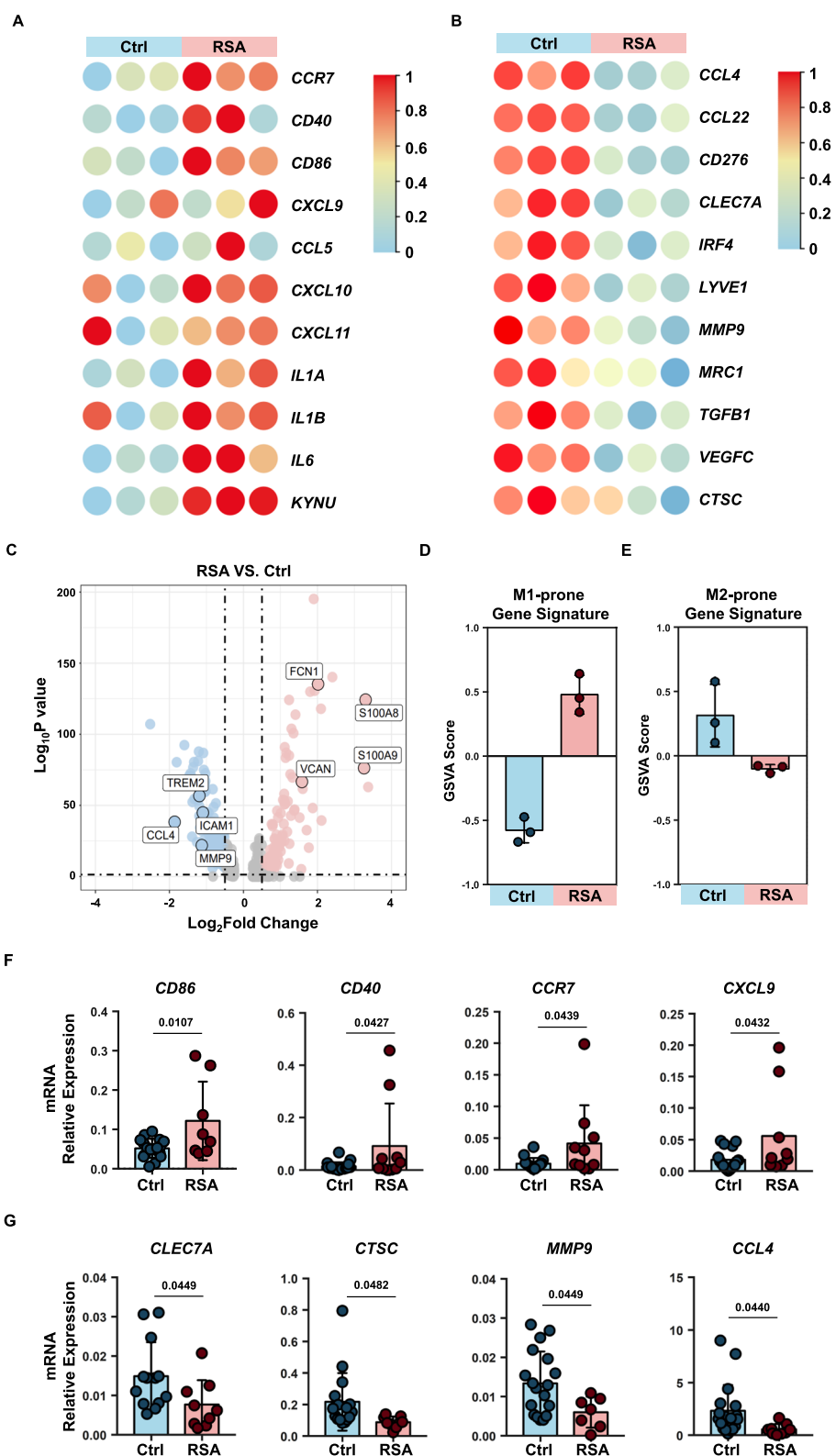
Chen *et al. Journal of Translational Medicine*   (2024) 22:1017

Page 8 of 18

Fig. 2 (See legend on previous page.)

Chen *et al. Journal of Translational Medicine*   (2024) 22:1017

Page 9 of 18

Furthermore, we examined the gene expression levels of other M1 phenotype markers, such as IL1B, IL6, and TNF. The results revealed a significant decrease in the gene expression levels of these molecules after coculture with dNK cells (Fig. 3F).

Altogether, these findings indicate that decidual NK cells from normal pregnancy have the capacity to induce a transition from an M1 phenotype to an M2 phenotype in decidual macrophages. The specific molecular mechanisms underlying this functionality warrant further investigation.

dNK cells from normal pregnancy express the natural ligand of VSIG4

Previously, VSIG4 has been reported to be highly expressed on M2 macrophages and tumor-associated macrophages (TAMs) [37–39]. PCR results revealed that the VSIG4 gene is also highly expressed in decidual macrophages from normal pregnancies. In contrast, its expression was nearly absent in decidual NK cells, peripheral blood NK cells, and monocytes (Fig. 4A). Additionally, we detected the expression of VSIG4 protein on the membrane surface of normal decidual macrophages using fluorescence staining (Fig. 4B).

We conducted RNA sequencing on peripheral blood NK cells and decidual NK cells and performed KEGG enrichment analysis to identify differential signaling pathways between the two. We found that, compared to peripheral NK cells, decidual NK cells were enriched in the complement and coagulation cascades pathway (Fig. 4C). Heatmap visualization of gene expression within this pathway revealed high expression of C3 in decidual NK cells (Fig. 4D). GSEA similarly showed enrichment of the complement and coagulation cascades pathway in genes highly expressed in decidual NK cells (Fig. 4E). Notably, C3 is cleaved to produce C3b, which happens to be the natural ligand for VSIG4.

To validate C3 expression in decidual NK cells, we used qPCR to assess the mRNA expression of C3 in peripheral NK cells and decidual NK cells. The results indicated minimal expression of C3 in peripheral NK cells, whereas decidual NK cells exhibited significantly higher expression levels ($P < 0.001$) (approximately one percent of ACTIN expression level) (Fig. 4F). Additionally, we detected the expression of C3b protein on the surface of decidual NK cells (Fig. 4G, H). Under the same detection conditions, the average fluorescence intensity of C3b in peripheral NK cells was significantly lower than that in decidual NK cells ($P < 0.001$).

In summary, normal decidual macrophages exhibit specific expression of VSIG4, while normal decidual NK cells express its natural ligand, C3b. These findings suggest a potential interaction between VSIG4 and C3b in the decidual immune microenvironment.

Weakened LFA1-C3 axis in dNK cells of RSA patients

Analysis of RNA sequencing data from decidual immune cells of RSA patients and normal pregnancies revealed a significant downregulation of C3 gene expression in dNK cells from RSA patients ($P = 0.0272$) (Fig. 5A, B). This phenomenon was further validated by qPCR results ($P = 0.0134$) (Fig. 5C). Western blot analysis was performed to assess the expression levels of C3b protein fragments in dNK cells from normal pregnancies and RSA patients. The results showed a significant decrease in the expression of C3b protein fragments in dNK cells from RSA patients, while dNK cells from normal pregnancies exhibited relatively high expression (Fig. 5D, E).

Previous reports have suggested that during T-cell extravasation from blood vessels into tissues, ICAM1 on endothelial cells can induce the upregulation of C3 mRNA within T cells by binding to LFA-1 on the T cell [40]. To investigate whether ICAM1 could also induce C3 mRNA expression in dNK cells, we added ICAM1 protein to the culture system of dNK cells. We observed a slight but significant upregulation of C3 mRNA in dNK cells from normal pregnancies in response to ICAM1 treatment. This trend could be reversed by the endogenous inhibitor of LFA1-ICAM1 binding, DEL-1 [41] (Fig. 5F), suggesting that the mechanism inducing C3 expression is applicable to dNK cells. We hypothesized that the expression of C3 mRNA in dNK cells is induced through their interaction with ICAM1-expressing decidual macrophages.

Previous studies have shown that LFA-1 is highly expressed by decidual NK cells in normal pregnant

(See figure on next page.)
Fig. 3 dNK cells from normal pregnancy inhibit pro-inflammatory macrophages. **A** Schematic representation of macrophage induction and co-culture system. **B** Flow cytometry plots depicting distinct subsets of induced macrophages. **C**, **D** Representative histogram (left) and expression level (right) of CD80 (**C**) or CD206 (**D**) in macrophages after co-culture with dNK cells from normal pregnancies. Experiments were repeated for 5 independent times. P values have been determined by two-tailed paired t-test. **E** Microscopic images illustrating changes in the cellular morphology of M1 macrophages following co-culture with dNK cells. Scale bar = 100 μm. **F** Gene expression levels of IL1B, IL6, TNF, and CD80 in macrophages co-cultured with normal pregnancy dNK cells. Experiments were repeated for 3 independent times. P values have been determined by two-tailed unpaired t-test
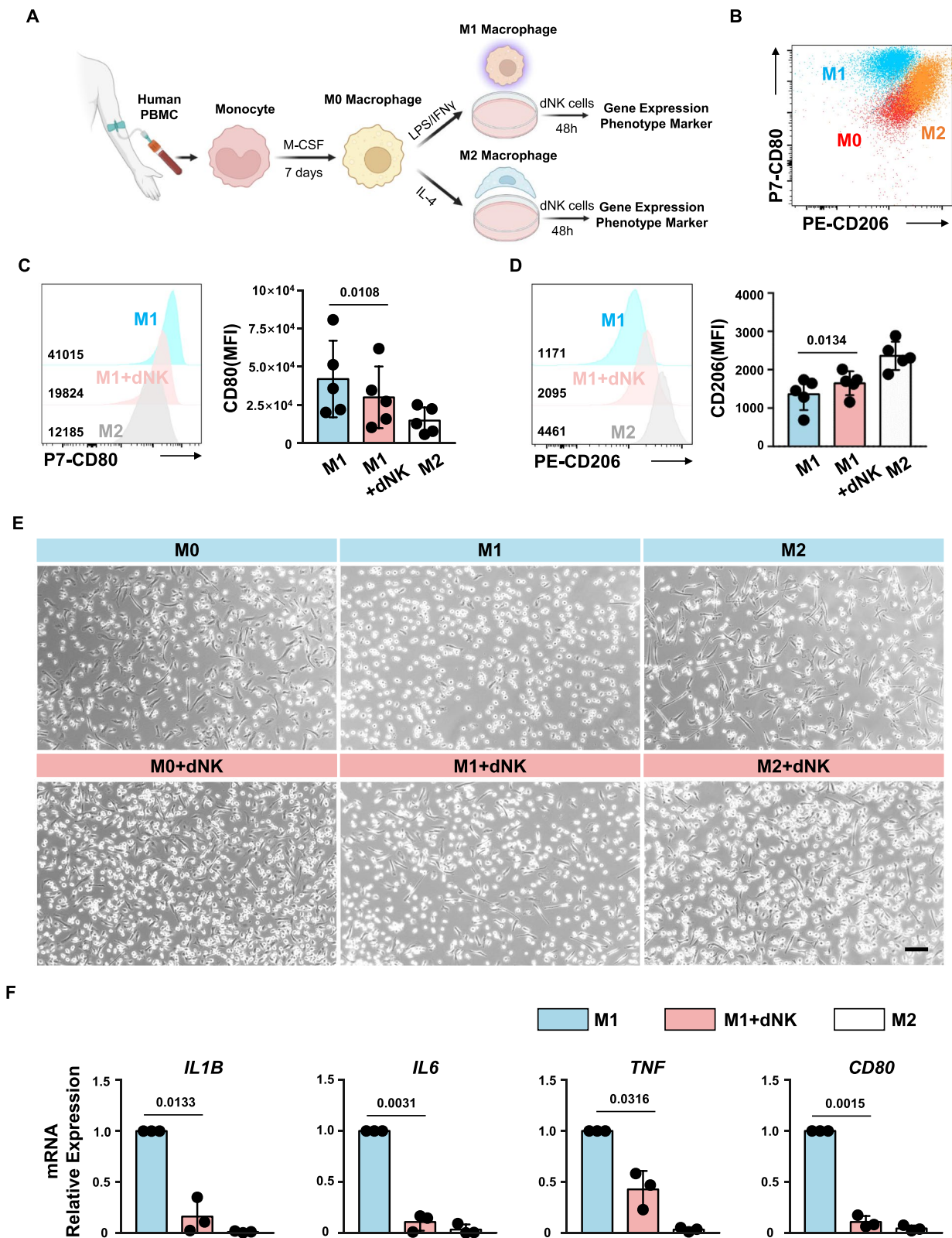
Chen *et al. Journal of Translational Medicine* (2024) 22:1017

Page 10 of 18

Fig. 3 (See legend on previous page.)

women [42]. To investigate whether the reduced expression of C3 in dNK cells from RSA patients is due to a defect in the abovementioned mechanism, we examined the expression levels of LFA-1 in normal and RSA patient dNK cells. We found that LFA1+ dNK cells were significantly reduced in the decidual tissue of RSA patients (*P* < 0.001) (Fig. 5G and H). These data suggest that dNK cells from RSA patients exhibit lower levels of C3b, the natural ligand of VSIG4, than normal dNK cells, and their C3 mRNA expression levels are also lower than those in normal dNK cells. The reduced expression of C3 mRNA is attributed to the diminished proportion of LFA1+ dNK cells in RSA patients, resulting in a compromised ICAM1-LFA1 signaling axis that induces C3 mRNA expression.

VSIG4 blockade impairs C3b-induced macrophage polarization.

To investigate the expression of ICAM1 signaling upstream of LFA1-C3 in decidual macrophages and validate the hypothesis that C3 expression in dNK cells is induced by ICAM1 in macrophages, we analyzed previously published single-cell data of decidual macrophages [9]. Our analysis revealed a significant reduction in ICAM1 expression in decidual macrophages from RSA patients compared to those from normal pregnancies (Figs. 2 and 6A, B). Additionally, the expression of VSIG4, indicative of an M2 phenotype, was significantly lower in decidual macrophages from RSA patients, consistent with our previous findings. These results were further validated by qPCR and immunofluorescence assays (Fig. 6C–E).

To confirm the existence of the ICAM-LFA1 ligand–receptor relationship in the decidual microenvironment and that the M2 phenotype of normal decidual macrophages is maintained through the C3b-VSIG4 axis, we introduced a blocking antibody against VSIG4 into the coculture system presented in Fig. 3A. As hypothesized, blocking VSIG4 partially reversed the phenotypic transition of normal decidual NK cells from M1 macrophages to M2-like cells upon coculture with dNK cells (Fig. 6F and G). This suggests that the function of dNK cells in

this context is not solely achieved through this ligand–receptor pair and may involve other ligands or soluble cytokines.

These data demonstrate that decidual macrophages in normal pregnancy can induce high C3 expression in LFA1+ decidual NK cells through ICAM1 signaling. These NK cells, in turn, maintain an M2-like phenotype in macrophages through the binding of C3b to macrophage surface VSIG4. In the decidual microenvironment of RSA patients, the compromised ICAM-LFA1-C3b-VSIG4 signaling axis in macrophages leads to the inability to sustain the M2 phenotype, disrupting the immune homeostasis of the decidual microenvironment.

Previous reports have indicated that the C3 protein in tissue T cells is cleaved by intracellular cathepsin L into active C3a and C3b fragments [43]. However, our RNA sequencing data revealed that cathepsin L was almost nonexistent in both pNK and dNK cells (Fig. 7A). Therefore, it is highly unlikely that the C3 protein in dNK cells is cleaved by CTSL. Interestingly, another proteinase within the same family as cathepsin L, cathepsin W [44, 45], showed significantly high expression levels in dNK cells (Fig. 7A and D).

To assess the potential binding between CTSW and C3, we employed ZDOCK to predict the molecular docking model for the interaction between CTSW and C3 (Fig. 7B, C). The binding region exhibited a mutual interaction surface area of 859.1 Å^2, with a binding energy of − 7.0 kcal/mol, indicating a stable binding affinity between the two proteins. The cyclic structural domain of CTSW complemented residues 73–80 of C3. Specifically, CTSW Pro321 formed a small hydrophobic region with the C3 A chain Glu73, resulting in the cleavage of the C3 protein into two parts, starting from the ANA structural domain of the C3 A chain (residues 1–77), which was detached to form the C3a fragment. Additionally, CTSW Pro317 formed a hydrogen bond with C3 A chain Arg80, facilitating the decomposition of Arg80 by CTSW and the formation of the N-terminal region of C3b, spanning residues 80–98. Molecular docking analysis revealed a stable binding affinity between CTSW and C3, with specific interactions involving the cyclic structural domain

(See figure on next page.)

Fig. 4 dNK cells from normal pregnancy express the natural ligand of VSIG4. **A** Gene expression levels of VSIG4 in peripheral blood NK cells (pNK), peripheral blood monocytes (pM), decidual macrophages (dM), and decidual NK cells (dNK). **B** Fluorescence image depicting the expression of VSIG4 protein on decidual macrophages. **C** Biological processes that are significantly enriched in Sankey dot pathway enrichment analysis of the upregulated genes of dNK relative to pNK. **D** Heat map of differential genes in complement and coagulation cascade pathways, n = 3 per group. **E** Gene set enrichment analysis (GSEA) revealed an increase in complement and coagulation cascade pathways (enrichment plot: COMPLEMENT AND COAGULATION CASCADES PATHWAYS, HSA04610) in dNK cells compared with pNK cells, n = 3 per group. **F** qPCR validation of the differential expression of the C3 gene in dNK cells and pNK cells. **G** CLSM images showing the secretion of C3b in pNKs and dNKs. The images were captured using the same parameters. Scale bars = 5 µm. **H** Statistical histogram of C3b mean fluorescence intensity of each decidual or peripheral NK cell. P values have been determined by two-tailed unpaired t-test
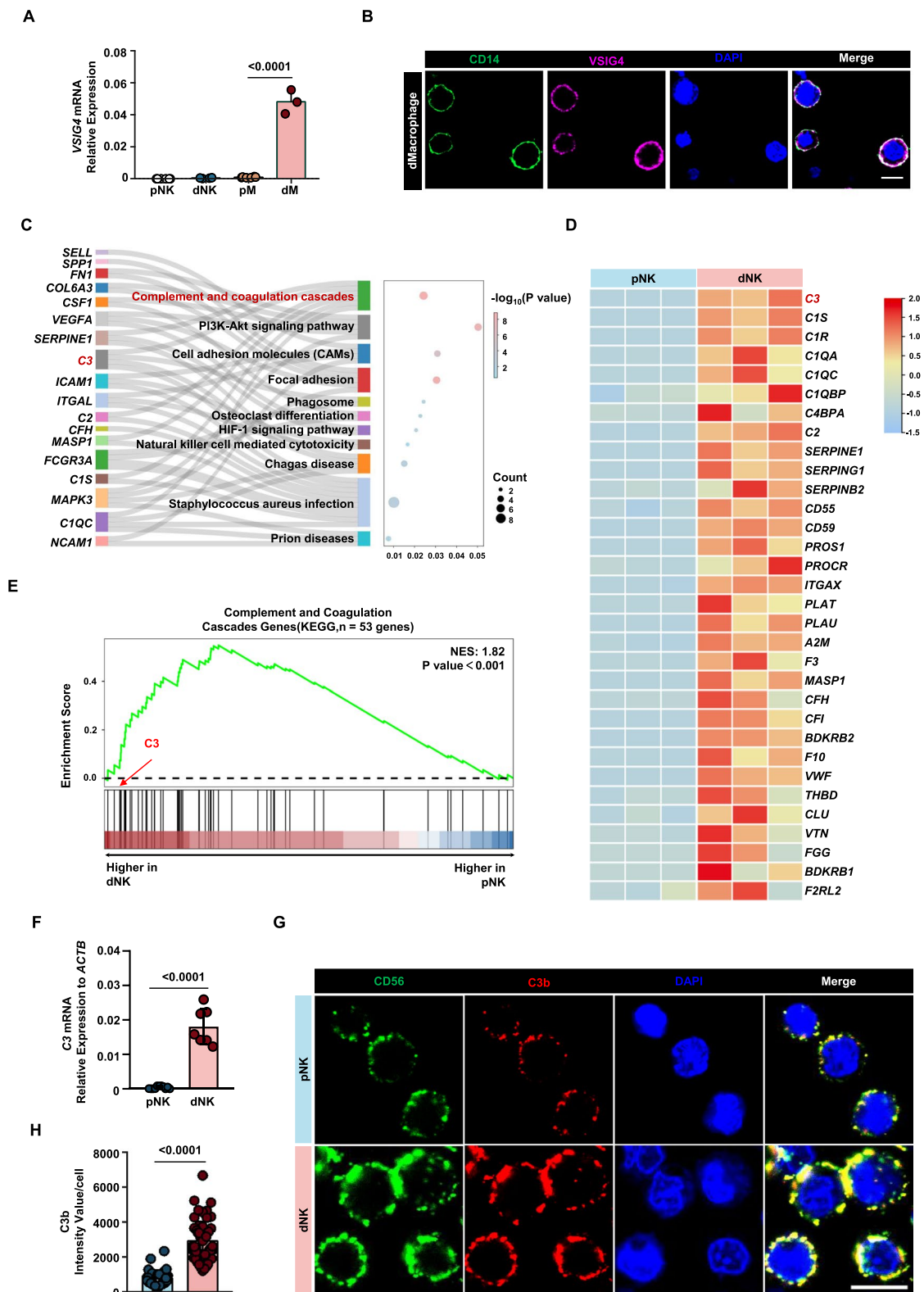
Chen *et al. Journal of Translational Medicine*   (2024) 22:1017

Page 12 of 18
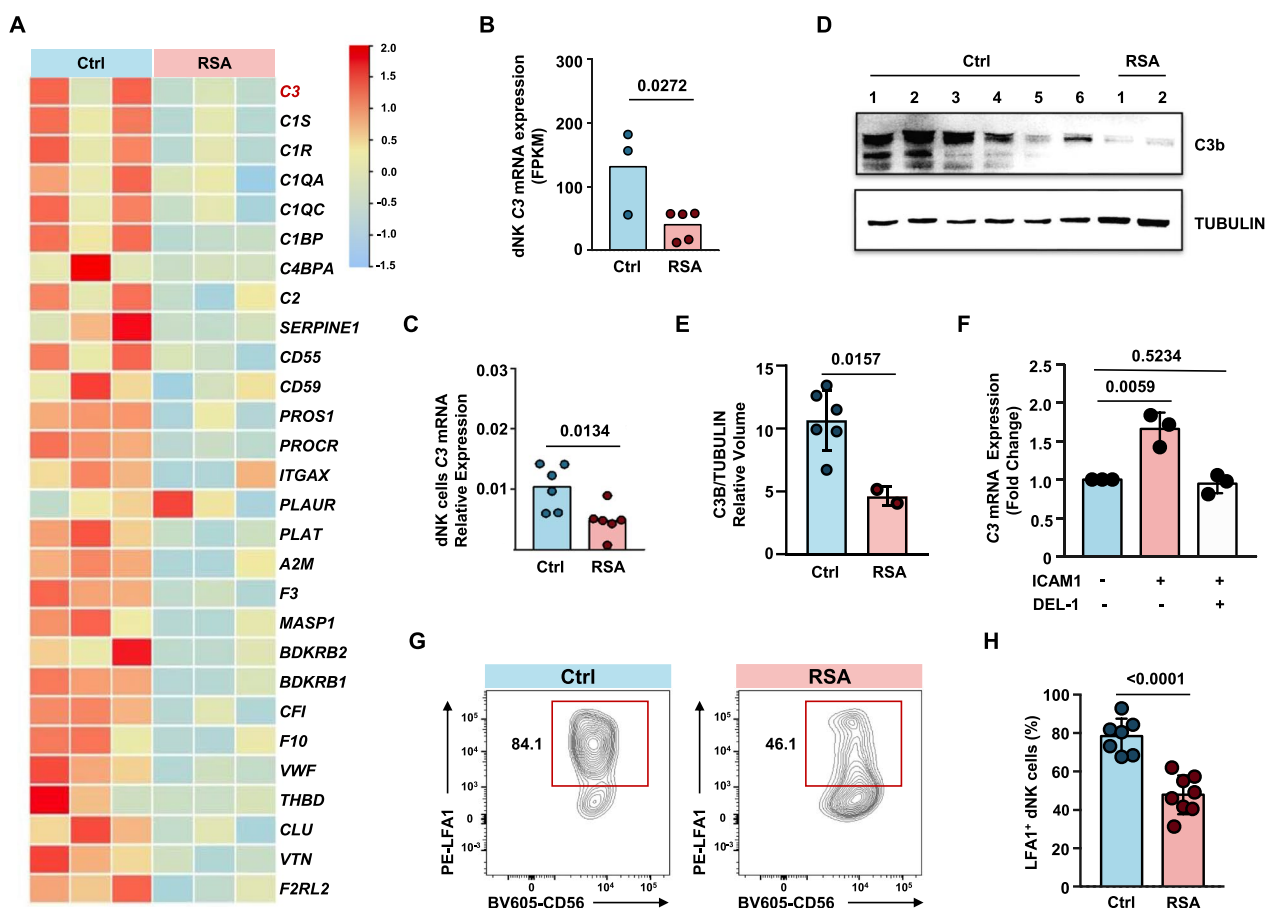

Fig. 4 (See legend on previous page.)

Fig. 5 Weakened LFA1-C3 signaling in dNK cells in RSA patients. **A** Heat map of differential genes in complement and coagulation cascade pathways, n = 3 per group. **B** Comparison of FPKM values of C3 (complement C3) in dNK cells from RNA-seq data. Unpaired t-test. **C** qPCR assessment of C3 gene expression levels in decidual NK cells from normal pregnancies and RSA patients (n = 6 per group). **D** Western blot analysis of C3 protein expression levels in decidual NK cells from normal pregnancies and RSA patients. **E** Relative volume quantification of C3B protein and the internal control protein TUBULIN using ImageLab software. **F** qPCR analysis of C3 gene expression in dNK cells stimulated with ICAM1 protein, or co-stimulated with ICAM1 protein and the LFA1-ICAM1 binding blocking protein DEL-1 for 24 h. **G** Representative contour plots of LFA1+ dNK cells gated on CD45+CD3−CD56+ cells. **H** Statistical chart presenting the proportions of LFA1+ dNK cells across normal pregnancies group and RSA group. P values have been determined by two-tailed unpaired t-test

(See figure on next page.)
Fig. 6 VSIG4 blockade impairs C3b induced macrophages polarization. **A** Uniform manifold approximation and projection (UMAP) of single-cell RNA-seq from human decidual immune cells isolated from patients with RSA and healthy controls. The single-cell RNA sequencing data used in this study were previously published by Guo [9]. **B** Feature plot showed ICAM1 and VSIG4 expression in the different clusters between Ctrl vs. RSA as defined in (**A**). **C** Gene expression levels of VSIG4 and ICAM1 in decidual macrophages from normal pregnancies and RSA patients. **D** CLSM images showing the expression of VSIG4 protein in decidual macrophages from normal pregnancies and RSA patients. Scale bars = 5 μm. **E** Statistical histogram of VSIG4 mean fluorescence intensity of each decidual macrophages from normal pregnancies (n = 3) and RSA patients (n = 3). **F** Gene expression levels of IL1B, IL6 and TNF in macrophages with or without the addition of VSIG4 blocking antibody during co-culture with dNK. **G** Representative mean fluorescence intensity of CD80 (upper panel) or CD206 (lower panel) in macrophages with or without the addition of VSIG4 blocking antibody during co-culture with dNK. Experiments were repeated for 3 independent times. P values have been determined by two-tailed paired t-test

of CTSW and residues 73–80 of C3, ultimately leading to the cleavage and formation of C3a and C3b fragments.

The significantly elevated expression of CTSW in normal pregnancy decidua NK cells, coupled with the near absence of CTSW expression in RSA patient decidua (Fig. 7E–G), suggests that the reduced presence of the C3b fragment in RSA patient NK cells may be attributed to insufficient levels of the cleavage enzyme CTSW. These
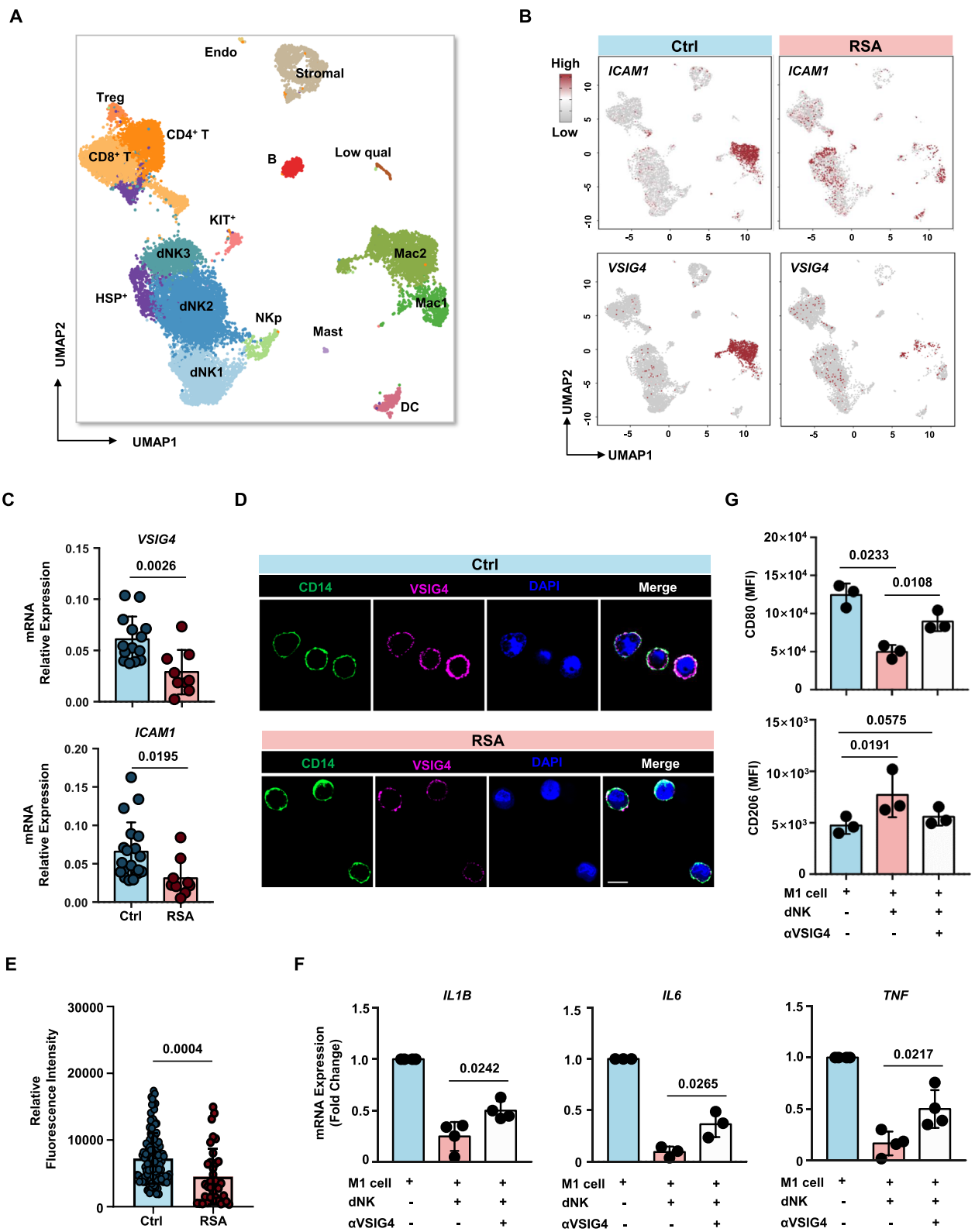
Chen *et al. Journal of Translational Medicine*   (2024) 22:1017

Page 14 of 18

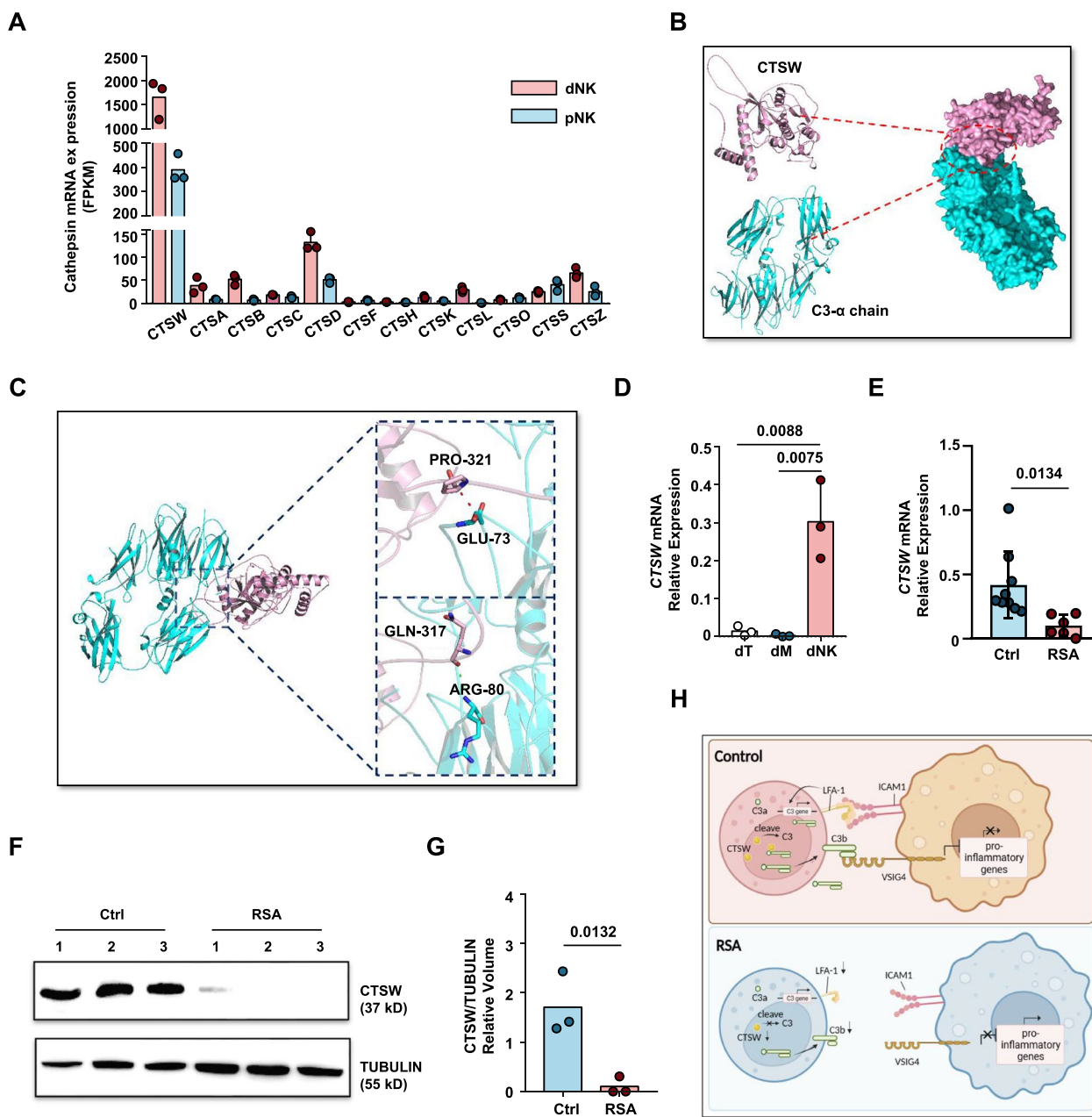**Fig. 6** (See legend on previous page.)

Fig. 7 C3 cleavage potential of cathepsin W. **A** FPKM values of cathepsin family genes in pNK cells and dNK cell RNA-seq data. **B** Schematic representation of the interaction between CTSW protein and C3 α-chain protein. **C** Schematic enlargement of the binding site between CTSW protein and C3 α-chain protein as simulated by ZDOCK. **D** Gene expression levels of CTSW in the three major immune cell subtypes of the decidua: NK cells, macrophages, and T cells. **E** Gene expression levels of CTSW in decidua NK cells from normal pregnancy and RSA patients. **F** Western blot analysis of CTSW protein expression in decidua NK cells from normal pregnancy and RSA patients, TUBULIN expression was measured as loading control. Experiments were repeated for 2 independent times. **G** Relative volume quantification of CTSW protein and the loading control protein TUBULIN using ImageLab software. **H** Graphic abstract of this article. Created with BioRender.com

findings suggest that C3 in dNK cells may undergo cleavage by CTSW, and the absence of CTSW in RSA patient dNK cells is another contributing factor to the reduced levels of the C3b fragment (Fig. 7H).

Discussion

Recurrent spontaneous abortion (RSA) can result from various causes, including chromosomal abnormalities, reproductive tract anomalies, hormonal imbalances, autoimmune diseases, and endometrial disorders [48].

Chen *et al. Journal of Translational Medicine*   (2024) 22:1017

Page 16 of 18

However, the pathogenesis remains unclear in approximately 50% of RSA cases, which are classified as unexplained recurrent spontaneous abortion (URSA). Recent studies increasingly suggest that many cases of URSA are associated with immune factors. The decidual microenvironment is rich in immune cells, and the interactions between different types of immune cells, as well as between immune cells and stromal cells, are critical for maintaining immune balance at the maternal–fetal interface. As the most abundant immune cells in the decidual microenvironment, NK cells play a crucial role in sustaining normal pregnancy. Abnormalities in the number or function of NK cells can lead to pregnancy failure. The mechanism by which abnormal decidual NK cell function contributes to recurrent spontaneous abortion has not yet been fully elucidated.

In this investigation, a substantial reduction in the interaction between decidual NK cells and macrophages within the decidual tissue of RSA patients compared to normal pregnancies was observed. This diminished contact persisted in an in vitro coculture system, indicating potential direct cell-surface receptor–ligand interactions between these cell types. Subsequent analyses of RNA-seq data and published single-cell sequencing data revealed an M1-prone gene expression profile in decidual macrophages from RSA patients, corroborated by qPCR. VSIG4, a B7 family-related protein known to be expressed on M2 macrophages in the tumor microenvironment or tumor-associated macrophages (TAMs), was detected in decidual macrophages from normal pregnancies, but its expression significantly decreased in RSA patients decidual macrophages. Concurrently, the natural ligand of VSIG4, C3b, was identified on decidual NK cells, suggesting a potential interaction through the C3b-VSIG4 axis. To investigate whether the C3b-VSIG4 axis could inhibit the proinflammatory phenotype of macrophages, decidual NK cells from normal pregnancies were cocultured with monocyte-induced M1 macrophages. The results demonstrated that decidual NK cells could suppress the proinflammatory phenotype of M1 cells. Importantly, this inhibitory effect could be partially reversed by a VSIG4-blocking antibody, indicating the existence of alternative induction mechanisms in addition to the C3b-VSIG4 axis.

Earlier studies have reported that T cells, upon extravasation into tissues, induce C3 mRNA transcription in tissue-localized T cells through the LFA1-ICAM1 interaction. Similarly, we observed a similar phenomenon in decidual NK cells, where C3 gene expression was much higher in these cells than in peripheral blood NK cells. This induction is likely mediated by ICAM1$^+$ decidual macrophages. Notably, cathepsin L, responsible for C3 cleavage in T cells, was nearly absent in decidual NK cells, suggesting an alternative mechanism for C3 cleavage. Molecular docking analysis proposed that another cathepsin family member, cathepsin W, may be responsible for C3 cleavage in dNK cells. Cathepsin W exhibited significantly elevated expression in normal pregnancy decidua NK cells but was nearly absent in RSA patient decidua. These findings suggest a potential role of CTSW in cleaving C3 in dNK cells and the absence of CTSW in RSA patient dNK cells may contribute to reduced levels of the C3b fragment. In contrast, RSA patient decidual NK cells, characterized by low expression of LFA1, are unable to efficiently induce the expression of C3 mRNA. Moreover, the expression level of cathepsin W in these cells was significantly lower than that in normal pregnancy dNK cells. These factors collectively result in significantly reduced production of C3b compared to normal levels, which, in turn, fails to provide an adequate ligand source for VSIG4. Consequently, this deficiency disrupts the phenotypic characteristics of macrophages in RSA patients.

In summary, this study uncovers a direct regulatory mechanism of decidual NK cells on decidual macrophages through the intracellular complement system, providing a potential pathogenic mechanism for recurrent spontaneous abortion. It is noteworthy that, in another study, a subset of recurrent spontaneous abortion cases was attributed to insufficient dNK cell numbers. In the cases presented in this article, the proportion of NK cells was not significantly reduced, but their phenotype appeared to be abnormal.

However, several issues in this study remain to be addressed. First, the phenomena observed in this study need to be validated in a larger cohort of patients with recurrent spontaneous abortion. Additionally, determining how to clinically intervene to enhance the expression of complement C3 or Cathepsin W in decidual NK cells to treat recurrent spontaneous abortion remains a challenge. This may require further investigation of the upstream signaling pathways of C3 in a mouse model.

Supplementary Information

Supplementary Material 1.

Supplementary Material 2.

Supplementary Material 3.

Author contributions
H.W., B.F., and S.C. conceived and conducted the project. H.W. supervised the project. S.C. and H.W. wrote the manuscript. S.C. carried out the experiments and data analysis. J.Z. contributed to the bulk RNA-seq and single cell RNA-seq

Chen *et al. Journal of Translational Medicine*   (2024) 22:1017

Page 17 of 18

data analysis. J.C., J.K., X.D. and Y.H. contributed to the sample collection. All authors reviewed the manuscript.

Availability of data and materials
The raw sequence data reported in this paper have been deposited in the Genome Sequence Archive (Genomics, Proteomics & Bioinformatics 2021) [46] in National Genomics Data Center (Nucleic Acids Res 2022 [47]), China National Center for Bioinformation/Beijing Institute of Genomics, Chinese Academy of Sciences (GSA-Human: HRA007005) that are publicly accessible at https://ngdc.cncb.ac.cn/gsa-human. The data that support the findings of this study are available from the corresponding author, H.W., upon reasonable request.

Declarations

Ethics approval and consent to participate
All human samples used in the present study were obtained under the approval of the Ethics Committee of the University of Science and Technology of China (2022KY-015; Hefei, China).

Competing interests
The authors declare no potential conflicts of interest.

References

1. Trundley A, Moffett A. Human uterine leukocytes and pregnancy. Tissue Antigens. 2004. https://doi.org/10.1111/j.1399-0039.2004.00170.x.
2. Bulmer JN, Williams PJ, Lash GE. Immune cells in the placental bed. Int J Dev Biol. 2010;54:281–94. https://doi.org/10.1387/ijdb.082763jb.
3. Koopman LA, et al. Human decidual natural killer cells are a unique NK cell subset with immunomodulatory potential. J Exp Med. 2003;198:1201–12. https://doi.org/10.1084/jem.20030305.
4. Manaster I, Mandelboim O. The unique properties of uterine NK cells. Am J Reprod Immunol. 2010;63:434–44. https://doi.org/10.1111/j.1600-0897.2009.00794.x.
5. Hanna J, et al. Decidual NK cells regulate key developmental processes at the human fetal-maternal interface. Nat Med. 2006;12:1065–74. https://doi.org/10.1038/nm1452.
6. Fu B, et al. Natural killer cells promote fetal development through the secretion of growth-promoting factors. Immunity. 2017;47:1100-1113.e6. https://doi.org/10.1016/j.immuni.2017.11.018.
7. Zhou Y, et al. PBX1 expression in uterine natural killer cells drives fetal growth. Sci Transl Med. 2020;12: eaax1798. https://doi.org/10.1126/scitranslmed.aax1798.
8. Von Woon E, et al. Number and function of uterine natural killer cells in recurrent miscarriage and implantation failure: a systematic review and meta-analysis. Hum Reprod Update. 2022;28:548–82. https://doi.org/10.1093/humupd/dmac006.
9. Guo C, et al. Single-cell profiling of the human decidual immune microenvironment in patients with recurrent pregnancy loss. Cell Discov. 2021;7:1. https://doi.org/10.1038/s41421-020-00236-z.
10. Zhang Y-H, He M, Wang Y, Liao A-H. Modulators of the balance between M1 and M2 macrophages during pregnancy. Front Immunol. 2017;8:120. https://doi.org/10.3389/fimmu.2017.00120.
11. Sayama S, et al. Human decidual macrophages suppress IFN-γ production by T cells through costimulatory B7–H1:PD-1 signaling in early pregnancy. J Reprod Immunol. 2013;100:109–17. https://doi.org/10.1016/j.jri.2013.08.001.
12. Mor G, Cardenas I, Abrahams V, Guller S. Inflammation and pregnancy: the role of the immune system at the implantation site. Ann N Y Acad Sci. 2011;1221:80–7. https://doi.org/10.1111/j.1749-6632.2010.05938.x.
13. Jaiswal MK, et al. V-ATPase upregulation during early pregnancy: a possible link to establishment of an inflammatory response during preimplantation period of pregnancy. Reproduction. 2012;143:713–25. https://doi.org/10.1530/REP-12-0036.
14. Vacca P, et al. Crosstalk between decidual NK and CD14⁺ myelomonocytic cells results in induction of Tregs and immunosuppression. Proc Natl Acad Sci USA. 2010;107:11918–23. https://doi.org/10.1073/pnas.1001749107.
15. Vondra S, Höbler AL, Lackner AI, Raffetseder J, Mihalic ZN, Vogel A, Saleh L, Kunihs V, Haslinger P, Wahrmann M, Husslein H. The human placenta shapes the phenotype of decidual macrophages. Cell Rep. 2023. https://doi.org/10.1016/j.celrep.2022.111977.
16. Li Z-H, et al. Galectin-9 alleviates LPS-induced preeclampsia-like impairment in rats via switching decidual macrophage polarization to M2 subtype. Front Immunol. 2018;9:3142. https://doi.org/10.3389/fimmu.2018.03142.
17. Wang L, et al. Decorin promotes decidual M1-like macrophage polarization via mitochondrial dysfunction resulting in recurrent pregnancy loss. Theranostics. 2022;12:7216–36. https://doi.org/10.7150/thno.78467.
18. Williams PJ, Searle RF, Robson SC, Innes BA, Bulmer JN. Decidual leucocyte populations in early to late gestation normal human pregnancy. J Reprod Immunol. 2009. https://doi.org/10.1016/j.jri.2009.08.001.
19. Yang H-L, et al. Decidual stromal cells maintain decidual macrophage homeostasis by secreting IL-24 in early pregnancy. Am J Reprod Immunol. 2020;84: e13261. https://doi.org/10.1111/aji.13261.
20. Zajac E, et al. Angiogenic capacity of M1- and M2-polarized macrophages is determined by the levels of TIMP-1 complexed with their secreted proMMP-9. Blood. 2013;122:4054–67. https://doi.org/10.1182/blood-2013-05-501494.
21. Gao CH, Dong HL, Tai L, Gao XM. Lactoferrin-containing immunocomplexes drive the conversion of human macrophages from M2- into M1-like phenotype. Front Immunol. 2018. https://doi.org/10.3389/fimmu.2018.00037.
22. Pierce BG, Hourai Y, Weng Z. Accelerating protein docking in ZDOCK using an advanced 3D convolution library. PLoS ONE. 2011;6: e24657. https://doi.org/10.1371/journal.pone.0024657.
23. Wu T, et al. clusterProfiler 4.0: a universal enrichment tool for interpreting omics data. Innovation. 2021;2:100141. https://doi.org/10.1016/j.xinn.2021.100141.
24. Zhang L, Li Z, Skrzypczynska KM, Fang Q, Zhang W, O'Brien SA, He Y, Wang L, Zhang Q, Kim A, Gao R. Single-cell analyses inform mechanisms of myeloid-targeted therapies in colon cancer. Cell. 2020. https://doi.org/10.1016/j.cell.2020.03.048.
25. Zheng GX, Terry JM, Belgrader P, Ryvkin P, Bent ZW, Wilson R, Ziraldo SB, Wheeler TD, McDermott GP, Zhu J, Gregory MT. Massively parallel digital transcriptional profiling of single cells. Nat Commun. 2017. https://doi.org/10.1038/ncomms14049.
26. Butler A, Hoffman P, Smibert P, Papalexi E, Satija R. Integrating single-cell transcriptomic data across different conditions, technologies, and species. Nat Biotechnol. 2018;36:411–20. https://doi.org/10.1038/nbt.4096.
27. Chen X, et al. Identification of FCN1 as a novel macrophage infiltration-associated biomarker for diagnosis of pediatric inflammatory bowel diseases. J Transl Med. 2023;21:203. https://doi.org/10.1186/s12967-023-04038-1.
28. Yang Q, et al. Single-cell RNA sequencing reveals the heterogeneity of tumor-associated macrophage in non-small cell lung cancer and differences between sexes. Front Immunol. 2021;12:756722. https://doi.org/10.3389/fimmu.2021.756722.
29. Krasniewski LK, et al. Single-cell analysis of skeletal muscle macrophages reveals age-associated functional subpopulations. Elife. 2022;11: e77974. https://doi.org/10.7554/eLife.77974.
30. Ganta VC, Choi M, Farber CR, Annex BH. Antiangiogenic VEGF165b regulates macrophage polarization via S100A8/S100A9 in peripheral artery disease. Circulation. 2019. https://doi.org/10.1161/CIRCULATIONAHA.118.034165.

Chen *et al. Journal of Translational Medicine*   (2024) 22:1017

Page 18 of 18

31. Park MD, et al. TREM2 macrophages drive NK cell paucity and dysfunction in lung cancer. Nat Immunol. 2023;24:792–801. https://doi.org/10.1038/s41590-023-01475-4.

32. Wu K, Byers DE, Jin X, Agapov E, Alexander-Brett J, Patel AC, Cella M, Gilfilan S, Colonna M, Kober DL, Brett TJ. TREM-2 promotes macrophage survival and lung disease after respiratory viral infection. J Exp Med. 2015. https://doi.org/10.1084/jem.20141732.

33. Luo Q, et al. TREM2 insufficiency protects against pulmonary fibrosis by inhibiting M2 macrophage polarization. Int Immunopharmacol. 2023;118:110070. https://doi.org/10.1016/j.intimp.2023.110070.

34. Ji K, et al. Integrating single-cell RNA sequencing with spatial transcriptomics reveals an immune landscape of human myometrium during labour. Clin Transl Med. 2023;13: e1234. https://doi.org/10.1002/ctm2.1234.

35. Ewa Z, et al. Angiogenic capacity of M1- and M2-polarized macrophages is determined by the levels of TIMP-1 complexed with their secreted proMMP-9. Blood. 2013. https://doi.org/10.1182/blood-2013-05-501494.

36. McWhorter FY, Wang T, Nguyen P, Chung T, Liu WF. Modulation of macrophage phenotype by cell shape. Proc Natl Acad Sci USA. 2013;110:17253–8. https://doi.org/10.1073/pnas.1308887110.

37. Huang X, et al. VSIG4 mediates transcriptional inhibition of Nlrp3 and Il-1β in macrophages. Sci Adv. 2019;5: eaau7426. https://doi.org/10.1126/sciadv.aau7426.

38. Li J, et al. VSIG4 inhibits proinflammatory macrophage activation by reprogramming mitochondrial pyruvate metabolism. Nat Commun. 2017;8:1322. https://doi.org/10.1038/s41467-017-01327-4.

39. Liu B, Cheng L, Gao H, Zhang J, Dong Y, Gao W, Yuan S, Gong T, Huang W. The biology of VSIG4: implications for the treatment of immune-mediated inflammatory diseases and cancer. Cancer Lett. 2023. https://doi.org/10.1016/j.canlet.2022.215996.

40. Kolev M, et al. Diapedesis-induced integrin signaling via LFA-1 facilitates tissue immunity by inducing intrinsic complement c3 expression in immune cells. Immunity. 2020;52:513-527.e8. https://doi.org/10.1016/j.immuni.2020.02.006.

41. Choi EY, et al. Del-1, an endogenous leukocyte-endothelial adhesion inhibitor, limits inflammatory cell recruitment. Science. 2008;322:1101–4. https://doi.org/10.1126/science.1165218.

42. Kopcow HD, et al. Human decidual NK cells form immature activating synapses and are not cytotoxic. Proc Natl Acad Sci USA. 2005;102:15563–8. https://doi.org/10.1073/pnas.0507835102.

43. Liszewski MK, et al. Intracellular complement activation sustains T cell homeostasis and mediates effector differentiation. Immunity. 2013;39:1143–57. https://doi.org/10.1016/j.immuni.2013.10.018.

44. Li J, et al. Cathepsin W restrains peripheral regulatory T cells for mucosal immune quiescence. Sci Adv. 2023;9: eadf3924. https://doi.org/10.1126/sciadv.adf3924.

45. Wex T, et al. Human cathepsin W, a cysteine protease predominantly expressed in NK cells, is mainly localized in the endoplasmic reticulum. J Immunol. 2001;1950(167):2172–8. https://doi.org/10.4049/jimmunol.167.4.2172.

46. Chen T, et al. The genome sequence archive family: toward explosive data growth and diverse data types. Genom Proteom Bioinform. 2021;19:578–83. https://doi.org/10.1016/j.gpb.2021.08.001.

47. Bao Y, Zhang Z, Zhao W, Xiao J, He S, Zhang G, Li Y, Zhao G, Chen R, Bu C, Zheng X. Database resources of the National Genomics Data Center, China National Center for Bioinformation in 2024. Nucl Acids Res. 2023. https://doi.org/10.1093/nar/gkad1078.

48. Dimitriadis E, Menkhorst E, Saito S, Kutteh WH, Brosens JJ. Recurrent pregnancy loss. Nat Rev Dis Prim. 2020;6:98.

Publisher's Note